

Ratiometric strategy assisted electrochemical detection of 4-nitrophenol in water samples using nanostructured CuO

Prakasam Sampathkumar ^{a, b}, Latha Chellamuthu Dilip Kumar ^a, Krishnan Giribabu ^{a, b},
Chinnathambi Suresh ^{a, b*}

^aElectrodics and Electrocatalysis Division, CSIR-Central Electrochemical Research Institute, Karaikudi-630 003, Tamil Nadu, India

^bAcademy of Scientific and Innovative Research (AcSIR), Ghaziabad- 201002, India

*Corresponding Author: Tel: 04565241338, Email: csuresh@cecri.res.in

(C. Suresh)

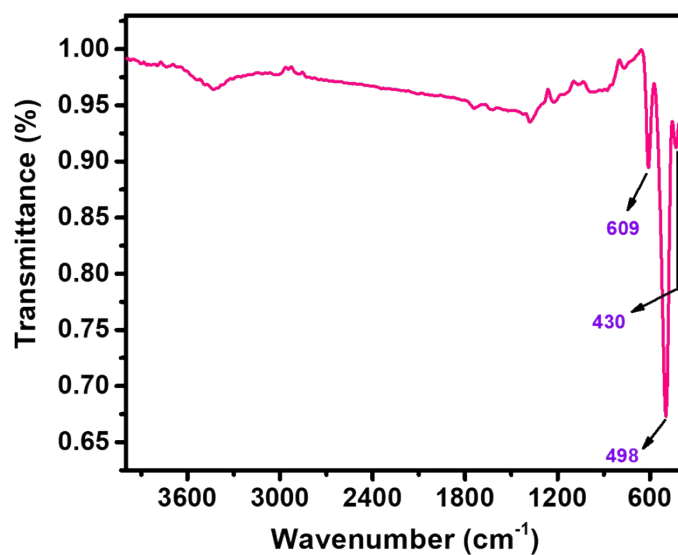


Fig. S1. FT-IR spectrum of CuO.

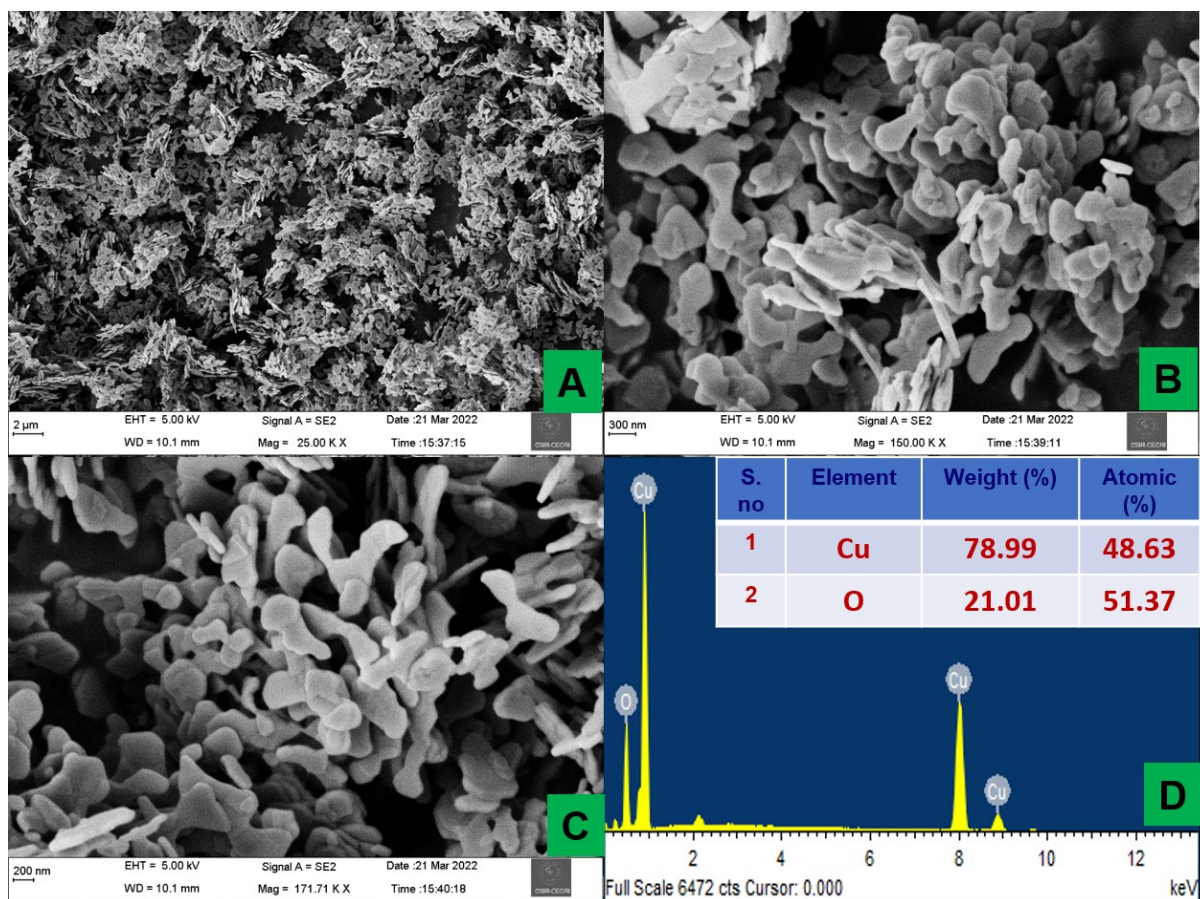


Fig. S2. FE-SEM images (A-C) and (D) EDAX of the prepared CuO.

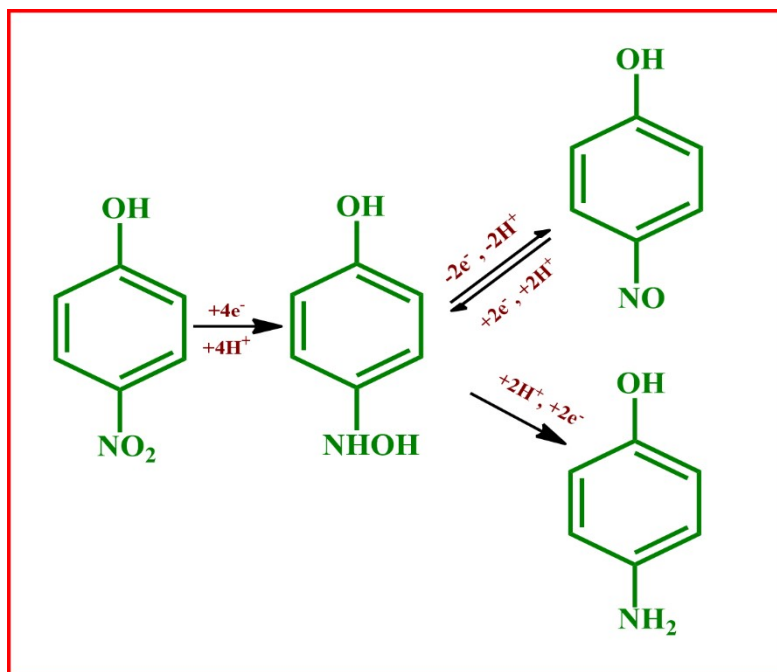


Fig. S3. Mechanism involved during 4-NP sensing.

Electrochemical impedance spectroscopy of GCE & CuO/GCE

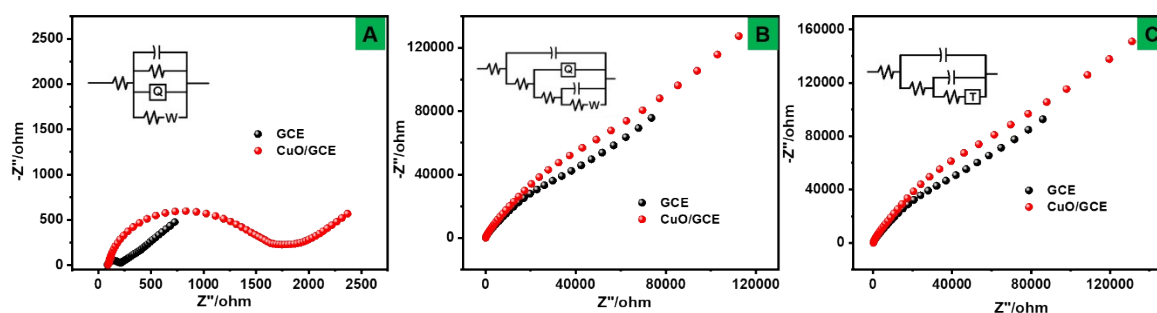


Fig. S4. EIS of bare GCE and CuO/GCE (A) in 5 mM $K_3Fe(CN)_6$ and $K_4Fe(CN)_6$ solution containing 0.1 M KCl, (B) in phosphate buffer solution (pH 7.4) and (C) phosphate buffer solution (pH 7.4) in presence of 1 mM 4-NP at a frequency range of 0.1 Hz to 100000 Hz.

(A). The R_{ct} value for Bare GCE is 140 Ω and CuO/GCE is 323 Ω .

(B). The R_{ct} values for Bare GCE is 113.2 Ω and CuO/GCE is 65.7 Ω .

(C). The R_{ct} value for Bare GCE is 466.2 Ω and CuO/GCE is 342.2 Ω

EIS was carried out under three different conditions: Fig. S4A. In the presence of 5 mM ferricyanide/ferrocyanide, Fig. S4B. In the presence of phosphate buffer, Fig. S4C. in the presence of 1 mM 4-NP in phosphate buffer. In the case of ferricyanide/ferrocyanide, CuO/GCE (323 Ω) exhibited higher R_{ct} compared to bare GCE (140 Ω). This might be due to the accumulation of a high flux of charges at the pores of CuO compared to bare GCE. The high accumulation charge may increase the R_{ct} . In the absence and presence of 4-NP, at the high-frequency range, both bare GCE and CuO /GCE exhibited similar behavior, but at the low-frequency range, CuO/GCE showed the charge transfer phenomena due to its hierarchy structure.

Electrochemical Active Surface Area (EASA) Measurement.

The EASA of the GCE and CuO/GCE have been calculated using the following Eq. 1.^[1]

$$EASA = \frac{C_{dl}}{C_s} \dots\dots\dots [1]$$

C_{dl} is the double-layer capacitance calculated from Impedance spectroscopy, and C_s is the specific capacitance of GCE (0.027 mF). From these, the calculated EASA of GCE and CuO/GCE is 0.071 cm^2 and 0.087 cm^2 .

General electrochemical mechanism between CuO and 4-NP.

In general, transition metal-based electrode matrices have attracted much attention in electrochemical sensor applications. This is due to the unique structure and morphology, easy

surface modifications, rapid preparation, etc. The copper-based material possesses excellent properties among the various transition metals due to its multiple oxidation states. In connection with the electrochemical sensing of 4-NP, the prepared ink was drop cast on the GCE surface and kept for complete drying, the experiments were performed in the phosphate buffer solutions. The copper oxide with multiple oxidation states acts as a coordinating center for the analyte molecule 4-NP. Once, the 4-NP reaches the CuO surface through diffusion process, it may moderately bind the CuO surface. The electrons are ejected from the CuO surface by applying the external potential to the CuO/GCE. These ejected electrons will be utilized for the analytical signal of 4-NP (oxidation & reduction).

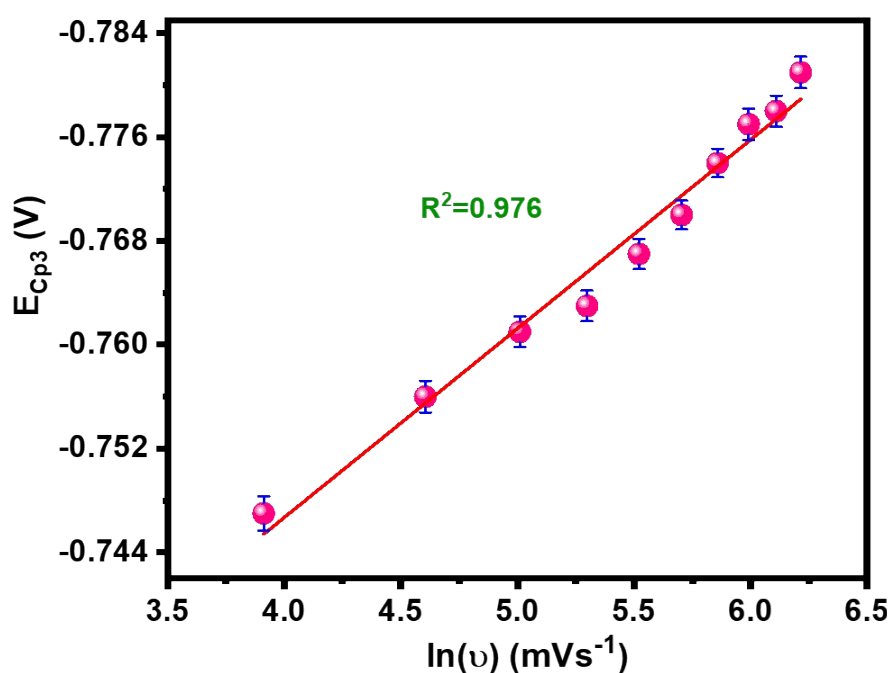


Fig. S5. E_{cp3} vs $\ln(v)$ plots for CuO/GCE.

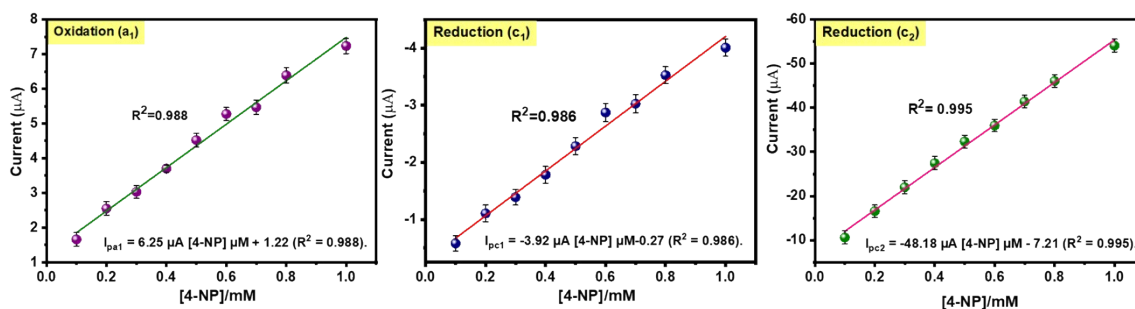


Fig. S6. Concentration studies linear plots for Bare GCE.

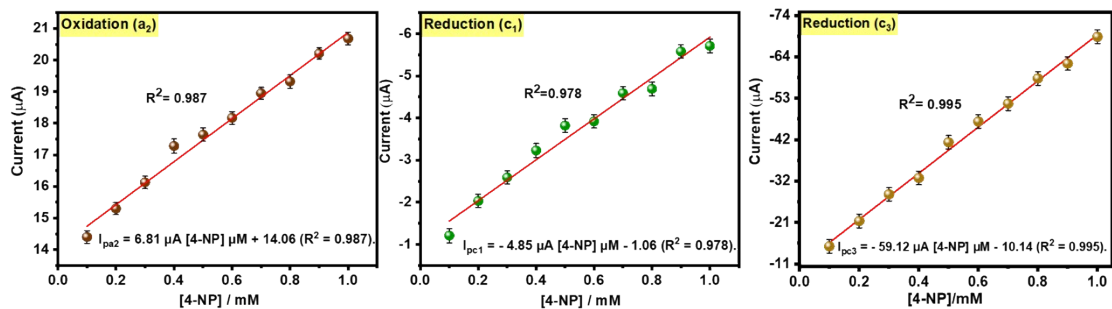


Fig. S7. Concentration studies linear plots for CuO/ GCE.

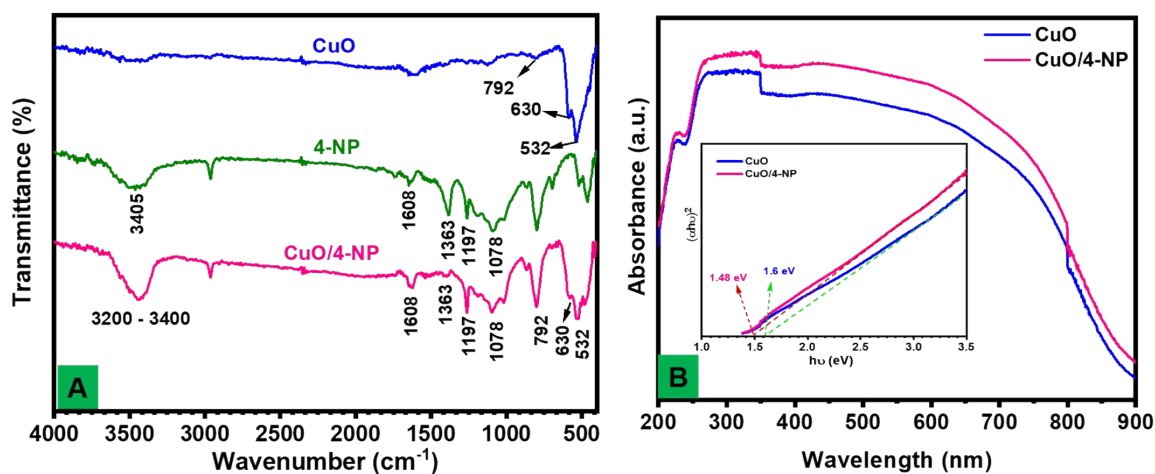


Fig. S8. (A) FT-IR spectrum of CuO,4-NP and CuO/4-NP and (B) DRS-UV and its corresponding Tauc plot of CuO and CuO/4-NP.

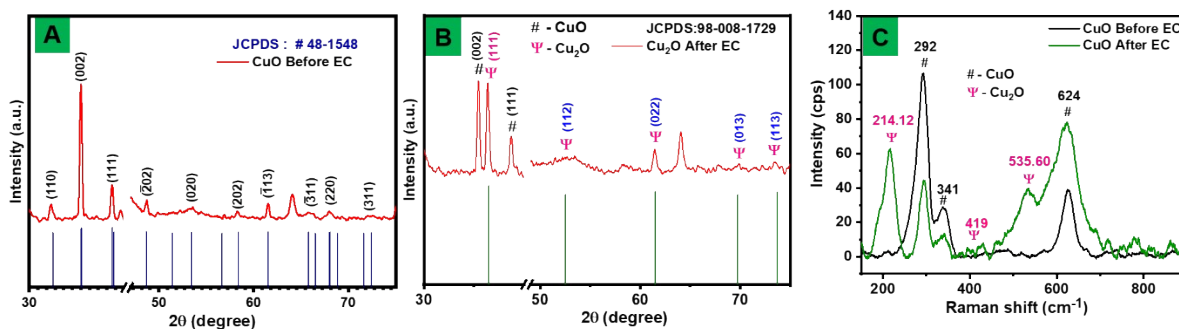


Fig. S9. Post analysis of CuO (A & B) XRD and (C) Raman spectroscopy.

Table. S1. Comparison of copper-based electrodes for 4-NP detection.

S. No	Electrodes	Techniques	Linear range (μM)	Limit of detection (μM)	References
01	Ni@CuO/rGO/PtE	DPV	0.09 – 105	0.0054	[2]
02	Cu _x -Fe ₃ O ₄ -VXC-72/GCE	DPV	0.1 – 4; 5 – 150	0.065	[3]
03	CeO ₂ -Cu ₂ O	CV	74 – 390	2.85	[4]
04	CeO ₂ -Cu ₂ O/CH	CV	74 – 375	2.03	[4]
05	CuBi ₂ O ₄	DPV	-	0.61	[5]
06	CeO ₂ :Cu NPs	CV	7.18 – 5000	7.18	[6]
07	Cu ₂ O sheets	DPV	6 – 2720	0.5	[7]
08	Cu(BTC)MOF@CNF	DPV	5.0 – 400	0.0871	[8]
09	SH- β -CD-RGO/Cu NSs	DPV	0.05 – 25; 25 – 100	0.02	[9]
10	Cu-MOF/NGO/SPCE	DPV	0.5 – 100	0.035	[10]
11	CNF/CuCrO ₂	DPV	1 – 150	0.022	[11]
12	CuO/GCE	DPV	1 – 1000; 20 – 200	0.055 & 0.118	This work

SPE – Screen Printed Electrodes, EIS – Electrochemical Impedance Spectroscopy, VXC-72 - conductive carbon black Vulcan XC-72, CH – Chitosan, CV – Cyclic voltammetry, CNF – Carbon Nanofibres, BTC - benzene 1,3,5-tricarboxylic acid, SH- β -CD - Cyclodextrin- β -SH.

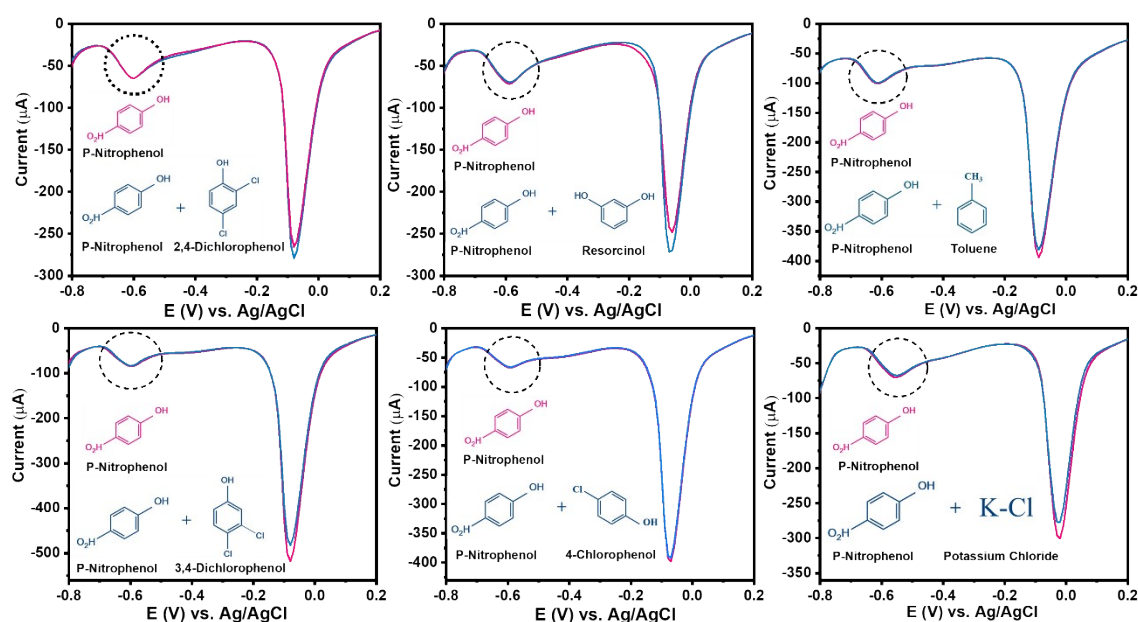


Fig. S10. DPV response of CuO/GCE in 0.1 M phosphate buffer (pH 7.4) having 50 μM of 4-NP with 500 μM of different interfering compounds.

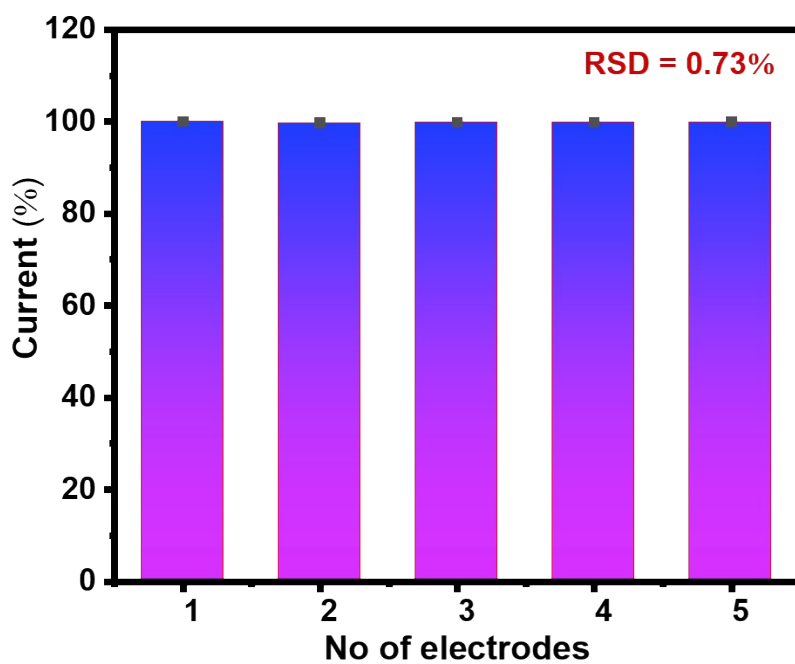


Fig. S11. Repeatability test, using five different CuO/GCE.

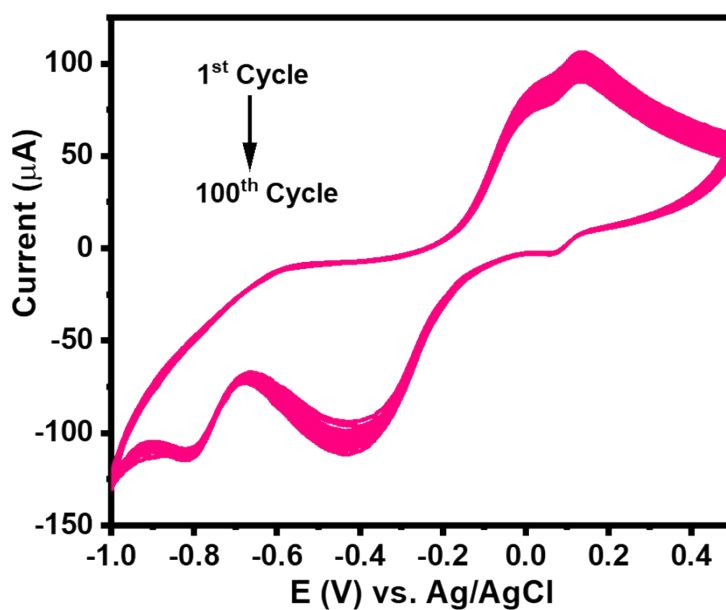


Fig. S12. Stability test for CuO/GCE.

References.

- [1] Z. Xie, W. Qu, E. A. Fisher, J. Fahlman, K. Asazawa, T. Hayashi, H. Shirataki and H. Murase, *Materials.*, 2024, **17**, 556.
- [2] J. Wu, K. Huang and L. Song, *Diam. Relat. Mater.*, 2024, **142**, 110829.
- [3] K. Cao, C. Si, H. Zhang, J. Hu and D. Zheng, *J. Mater. Sci. Mater. Electron.*, 2022, **33**, 2386–2398.
- [4] S. B. Khan, K. Akhtar, E. M. Bakhsh, and A. M. Asiri, *Appl. Surf. Sci.*, 2019, **492**, 726–735.
- [5] N. S. Gudipati, S. Vanjari, S. Korutla, R. R. Tammineni and S. Challapalli, *J. Environ. Chem. Eng.*, 2022, **10**, 108758.
- [6] A. A. Ansari and M. Alam, *J. Electroceramics*, 2021, **47**, 51–59.
- [7] V. Veeramani, M. Sivakumar, S. M. Chen, R. Madhu, Z. C. Dai, and N. Miyamoto, *Anal. Methods*, 2016, **8**, 5906–5910.
- [8] B. Dey, G. Sarkhel and A. Choudhury, *J. Macromol. Sci. Part A*, 2023, **60**, 150–160.
- [9] Z. Liu and Y. Guo, *J. Electroanal. Chem.*, 2018, **825**, 57–64.
- [10] A. D. Ambaye, K. K. Kefeni, T. G. Kebede, B. Ntsemdwana, S. B. Mishra and E. N. Nxumalo, *J. Electroanal. Chem.*, 2022, **919**, 116542.
- [11] S. Sakthinathan, R. Rajakumaran, A. K. Keyan, C. L. Yu, C. F. Wu, S. Vinothini, S. M. Chen and T. W. Chiu, *RSC Adv.*, 2021, **11**, 15856–15870.